Development of Biomass Derived Adsorbents using Wood Apple Pulp for the Removal of Contaminants

Surabhi S. Raj [1,2], Pooja Thanekar[1], Kshama Balapure[1], Vinay M. Bhandari*[1,2]

[1]Chemical Engineering and Process Development Division

CSIR-National Chemical Laboratory, Pune-411008, India

[2]Academy of Scientific and Innovative Research (AcSIR), Ghaziabad- 201002, India

*Email: vm.bhandari@ncl.res.in

Received: 15.3.2024, Revised: 20.4.2024, Accepted: 22.4.2024

Abstract

This study involves the development of biomass derived adsorbents from wood apple pulp for water and wastewater treatment. This biomass was modified by the addition of commercially available activated charcoal and copper nanoparticles. Adsorbent characterization was performed for understanding the surface morphology and surface area. These new adsorbents were further evaluated for their potentiality in removing dyes and API pollutants (Active Pharmaceutical Ingredient). All the adsorbents were highly effective in the removal of these contaminants, 96% of Malachite Green and 72% of Congo Red was removed with a high adsorption capacity of 45 mg/g. API pollutant (Ciprofloxacin) removal showed 52% removal, which is greater when compared to several modified adsorbents. Adsorption equilibrium models (Langmuir and Freundlich) and kinetic models (pseudo first order and pseudo second order) were evaluated for fit of the experimental data. In general, the isotherm studies indicated multilayer adsorption.

Keywords: *Adsorption, API pollutant, Characterization, Dye removal, Wood Apple*

DOI: 10.59143/isas.jisas.2.4.DNLJ2831

1. Introduction

Water plays an essential role in human life and it is necessary to fulfil the everyday requirements of every living being on this planet[1]. Several textile industries release toxic dyes and other organic pollutants into water and have known to be one of the most polluting industries of all. Growth of pharmaceutical industries, has led to the release of various antibiotics into natural water resources, and since their rate of entry into the environment is higher than their rate of elimination, they often tend to stay in water for long periods of time, hence referred to as pseudo-persistent. This persistence poses toxic effects on all living beings from microorganisms to humans[2]. Different treatment technologies, e.g. coagulation, adsorption, advanced oxidation processes, biological treatment, membrane separation etc. are practiced for the removal of various pollutants[3].Adsorption process is noted to be one of the most promising methodologies for the removal of organic pollutants existing in extremely low concentrations.

Large quantities of water and toxic chemicals are released from textile industries which are ultimately discharged into the water bodies in the form of effluents. Even the smallest quantity of dye can be clearly identified by their colour in the water streams[4]. Amongst various dyes, azo dyes like Malachite Green and Congo Red cause serious problems when released into water streams[5]. They exhibit carcinogenic and allergic properties which can cause adverse effects on aquatic and human lives[6,7]. Large scale production of antibiotics has led to migration of them into the environment causing pathogenic resistance, and extensive usage has led to the accumulation of these antibiotics in sediment, surface and groundwater[8]. Amongst several antibiotics Ciprofloxacin (CIP) was frequently identified in surface and wastewater with a concentration of 150 $\mu g\ L^{-1}$ in hospital effluents[9].

Several methods have been reported to remove dyes and low concentrations of API pollutants from water, out of which adsorption, membrane separation and coagulation are the most frequently used methods. Owing to its efficiency, availability, ease of operation and less cost, adsorption process using activated carbon materials is frequently used. It can be directly implemented into the treatment process, does not require any special design or condition and is capable of removing colour imparted from the toxic dyes at very low concentrations [10]. Usually in industries, commercially available activated carbon is used in treatment processes, but manufacturing and regeneration of it contributes to high costs. Significant research is being conducted on developing environmentally friendly low-cost biomass derived adsorbents which can replace the chemically synthesised activated carbon[11].

Several studies have been reported that show bio-based activated carbon materials are versatile in nature and can be used for various applications. Activated carbon derived from coffee waste and banana peel was used to remove Congo Red[12,]. Recent studies involving modified adsorbents such as prickly fruit pear and conductive polymer matrix have effectively removed Congo Red from water[13]. Different low-cost adsorbents derived from biomass prepared from *Borassus Flabellofer* (palm), *Lupinus Albus* seed peel, avocado fruit peel have been reported to remove Malachite Green dye from aqueous solutions[14]. Dao et al.[15] used several agricultural wastes such as straw, wood apple shell, banana peels, tea waste and avocado shells to remove Ciprofloxacin from water. Technological advances have allowed researchers to study biomass composites like methyl polysiloxane with avocado biochar and zinc oxide impregnated activated carbon prepared from jack fruit peel and their efficiency in removing Ciprofloxacin from aqueous solutions[16].

The present study was undertaken to evaluate the performance of biomass-derived adsorbents from ripened wood apple biomass for water and wastewater treatment. Adsorbent modifications were achieved by combining biomass with commercially available activated carbon to evaluate the efficiency when compared to pure biomass. Copper modified adsorbent was prepared by doping copper nanoparticles into a carbon matrix. The characterization of the adsorbents and efficacy was investigated with two case studies on the removal of dyes namely Malachite Green (MG) and Congo Red (CR) and one API pollutant Ciprofloxacin (CIP). The experimental data was fitted using the adsorption equilibrium models (Langmuir and Freundlich) and kinetic models (pseudo first order and pseudo second order). The present study reveals strategy for devising biomass-derived adsorbents for the utilization of easily available biomass which is a renewable material and can be sustainable/cost-effective alternative.

2. Materials and Methods

2.1 Materials

Ripened fruits of wood apple, were obtained locally from Pune, Maharashtra, India. The chemicals used were of analytical grade. Copper nanoparticles (Cu, 99.9%) were procured from the Nano Research Lab, India. Model dye pollutants used for adsorption studies were Malachite Green (MG) ($C_{52}H_{54}N_4O_{12}$; CAS No. 2437-29-8, MW:927.03, λ_{max}=617 nm, Thomas baker) and Congo Red (CR) ($C_{32}H_{22}N_6Na_2O_6S_2$; CAS No. 573-58-0, MW:696.65, λ_{max}=496 nm, Loba Chemie). For API pollutant removal studies, Ciprofloxacin

Hydrochloride Hydrate (CIP) ($C_{17}H_{18}FN_3O_3$.HCl, CAS No. 86393-32-0, MW:367.8, λ_{max}=275-282 nm, >98% purity, Sisco Research Laboratories Pvt. Ltd.) was used as a model pollutant. The commercial activated charcoal (powder form) was procured from Fluka. Spectroquant® Pharo 100 spectrophotometer (MERCK, India) was used for the measurement of Chemical oxygen demand (COD)/dye concentration. The samples were digested using Spectroquant® TR 320 (2 h at 148 °C). The Ciprofloxacin concentration was analysed using Agilent Technologies Cary 8454 (UV-Vis of wavelength range 200-800 nm).

2.2 Preparation of activated carbon from biomass

Ripened wood apple fruits were washed with distilled water and dried at room temperature. The inner pulp was scooped out from the outer hard shell for the preparation of different adsorbents. Different material modifications were performed as listed below:

a) Wood apple biomass (WA200): Fruit pulp was collected and coarsely ground using a regular mixer grinder. It was then dried at 60 °C in a hot air oven for 24 – 48 h to remove the moisture content. The biomass was then activated in a tube furnace employing inert gas atmosphere (nitrogen, flow rate 100 LPH) at 200°C for 4 hours. The sample was then collected, weighed and ground into a fine powder for further studies.

b) Wood apple biomass converted into activated carbon (WA350): Fruit pulp was collected and the previous steps were repeated. The dried biomass was then subjected to thermal treatment in a tube furnace in an inert atmosphere with nitrogen flow of 100 LPH at 350°C for 4 hours.

c) Wood apple biomass with activated charcoal (WAC200): The wood apple pulp was mixed appropriately with commercially available activated charcoal in 1:2 (activated charcoal: pulp) weight ratio. This step was performed to stabilise and preserve the natural compounds present in the pulp. The mixture was then dried at 60 °C for 24 – 48 h, activated in a tube furnace employing inert gas atmosphere (nitrogen, flow rate 100 LPH) at 200°C for 4 hours.

d) Wood apple biomass with activated charcoal converted into activated carbon (WAC350): This biomass was prepared using steps similar to WAC200. The dried mixture was then converted to activated carbon in a tube furnace in inert atmosphere at 350°C for 4 hours.

2.3 Preparation of copper bio nanocomposite

Wood apple ripened fruits were washed and dried at room temperature. The hard shell was then broken to collect the inner pulp which was ground coarsely in a mixer grinder. To this mixture 1% of copper nanoparticles were added. To partially remove the moisture content, the mixture was dried at 60 $^{\circ}$C. This dried material was subjected to thermal activation in an inert atmosphere at 350°C for 4 hours. Finally, the adsorbent, was named as WA-Cu for further convenience (Fig. 1).

2.4 Details of instrumentation for characterizing adsorbents

The adsorbent morphology was studied using field emission scanning electron microscope, FESEM (FEI Quanta 200, Netherlands; 3D dual beam with a resolution of 3nm at 30kV, tungsten filament as the electron source under high vacuum mode). Energy dispersive X-ray spectrometer, EDS (EDAX, AMETEK, Netherlands) was used for elemental analysis. Brunauer-Emmett-Teller (BET) (Quanta Chrome® ASiQwin^{TM} Autosorb, USA) was used for the surface area and pore size analysis. The pyrolysis process and the carbonisation temperatures were investigated by thermogravimetric analysis (TGA) (PerkinElmer STA 6000 simultaneous thermal analyser, USA). The identification of functional groups was done by Fourier transform infrared spectroscopy (FTIR) (FTIR-2000, PerkinElmer, Germany). Powder X-ray diffraction studies were carried out using X'Pert Pro PANalytical XRD (Netherlands) with Cu Kα radiation (λ = 1.542 Å) in 2θ range of 10–80°.

2.5 Experimental

2.5.1 Removal of Dyes and API pollutant

Batch experiments were performed to check the efficiency of the prepared adsorbents in removal of organic pollutants from water. Malachite Green and Congo Red were used as model dye systems and Ciprofloxacin Hydrochloride Hydrate was used as an API system for adsorption studies. An initial dye concentration of 50 ppm and API concentration of 20 ppm was used to perform experiments. Adsorbent dosage was fixed to be 0.1% in 20 ml of synthetic solutions of dye and API. Batch studies were conducted in an orbital shaker at a speed of 120 rpm for 16 h at pH ~6.5 and at the ambient temperature, 30±1°C. After filtering

out the adsorbents, the concentration of dye and API pollutants were determined from the absorbance values at wavelengths corresponding to wavelength of the dye/API which was pre-determined with the help of a UV-visible spectrophotometer. A similar procedure was followed for adsorption isotherm studies, but with different initial concentrations varying in the range of 10 – 100 ppm. COD analysis of the samples was performed before and after treatment to determine the amount of organic carbon present in the samples. Known amount of solutions A and B were added to the samples and digested for 2 hours at 148 $^{\circ}$C in a digester. After cooling, the samples were analysed in a previously programmed UV- visible spectrophotometer. The COD values were noted and % COD removal was calculated. Percentage removal and the amount of dye or API adsorbed per gram of adsorbent q_e (mg/g) was calculated as below:

$$\% \, removal = \frac{(Co - Ce)}{Co} \, X \, 100 \tag{1}$$

$$q_e = \frac{(C_0 - C_e) \times V}{m} \tag{2}$$

Where C_0 (mg/L) is the initial concentration of dye or API, C_e is the equilibrium concentration of dye or API, V is the volume (L) and m (g) is weight of the adsorbent.

3. Results and Discussion

3.1 Characterization of the adsorbents

Thermogravimetric analysis was performed to understand the stability of the samples at high temperatures and to understand the optimum temperature for thermal treatment. Fig. 2 represents TGA profiles of the samples. Mass of the sample was measured at corresponding temperatures up to 900 $^{\circ}$C in an inert atmosphere of nitrogen. From the thermogram it was observed that all the synthesised adsorbents have different degrees of stability. On an average, about 2% of moisture content was lost in the range of 50 to 100 $^{\circ}$C for all the samples and mostly all the volatile compounds get evaporated in this temperature range[17]. The disintegration of organic compounds like carbohydrates and proteins can be confirmed by the abrupt weight loss in all the samples[18]. The mass of WA-Cu remained constant upon increasing the temperature, this may be due to copper nanoparticles present in the material

that stabilise the carbon lattice structures. The weight loss has almost been halved in the case of all other adsorbents when compared to WA200. Thermal treatment and activated charcoal modifications might be the reason for higher stability. Above 250 °C maximum weight loss of 64.61% for WA200 was observed. WAC200 undergoes degradation and observed slight ash formation above 260 °C owing to 34.17% weight loss. These observations confirm that 200 °C is optimum for activation of WA200 and WAC200. WA350, WAC350 and WA-Cu undergo modifications after a temperature 400 °C. Hence, it can be concluded that a carbonisation temperature of 350 °C is desirable for the biomass derived activated carbon.

FE-SEM analysis provided a brief idea about the surface morphologies of different adsorbents. Surface of WA200 is moderately porous in nature and also consists of various porous cavities (Fig. 3a). This might be due to the activation of the material at 200 °C. It was confirmed that after carbonisation at 350 °C the pore size and shape of WA350 have been slightly modified (Fig. 3b). In case of biomass treated with activated charcoal, pores that were almost circular in shape, undergo slight modifications due to the presence of activated charcoal resulting in the formation of cylindrical pores (Fig. 3c). The surface of WAC200 is even when compared to raw biomass. This indicated that the number of pores has reduced, which in turn may decrease the adsorption capacities. Similar observations can be made in the case of WAC350 which consists of cylindrical pores, but due to carbonisation at 350 °C the pores are a lot more defined (Fig. 3d). Heterogeneous nature and random pore size distribution of the adsorbent can be observed in the case of WA-Cu (Fig. 3e). This is a reflection of copper nanoparticles present in the material. The presence of metal ions and irregular arrangement of the pores on the surface of the adsorbent might have led to better adsorption rates.

To find the elemental composition in the samples, EDAX analysis was performed. From the results obtained, it can be confirmed that carbon composition is higher in all the adsorbents compared to other elements like oxygen, calcium, phosphorous and potassium (Table 1). At the temperature of 200 °C carbon content in WA200 is 76.20%. Later on, increasing the temperature by 150 °C, it was observed that fixed carbon content in the samples have increased by 7%, and the composition of other elements like oxygen, phosphorous and potassium have drastically reduced. This is due to the evaporation of moisture content from the samples that remove almost all the volatile compounds leaving behind high carbon content[19]. In case of biomass treated with activated charcoal (WAC200 and WAC350), the

carbon content is much greater when compared to WA200 due to the presence of carbon moieties in charcoal. This might be the reason for drastic reduction in the oxygen content leading to lesser adsorption capacities. Copper-modified activated carbon can be distinguished clearly from other samples containing 2.24% copper, which indicates that copper has been adhered firmly to the raw material.

Brunauer-Emmett-Teller (BET) surface area analysis is a most essential technique to understand the surface characteristics of the adsorbents. Various parameters like surface area, pore volume and pore radius which are essential for adsorption studies can be deduced (Table 2). Clearly, it is observed that WA-Cu has higher pore size when compared to all other adsorbents and might be the reason for higher decolourisation. WA200, WA350 and WAC350 adsorbents have similar surface area which result in similar adsorption capacity and removal. Copper nanoparticles have enhanced the surface area and which is an important aspect for the removal of pollutants from water.

The FTIR spectrum presented a wide range of information on surface chemistry of the adsorbents. According to the data obtained, very few peaks are observed for all the adsorbents. This can be attributed to carbonisation, during which the carbon entities are eliminated in the form of CO_2. Due to this phenomenon, the available -OH and -COOH groups are typically broken down, resulting in only trace amounts being detected.

Different XRD patterns of the adsorbents are illustrated in Fig. 4. The combination of broad and sharp peaks represents the crystalline and amorphous nature of the adsorbents. A broad peak around 20^0 correspond to lattice planes of amorphous carbon[20]. Three sharp peaks around C (012), C (213) and C (241) planes attribute to crystalline graphitic carbon at 44^0 and 77^0. The crystalline nature alone manifests high purity and efficiency in material formation [21]. Weak bands around C (200) and C (231) at 38^0 and 64^0 contribute to the orthorhombic graphitic nature of carbon (JCPDS card No. 89-8490). Small peak at (122) plane confirms the presence of copper in WA-Cu which prevails in the form of copper oxide (JCPDS card No. 49-18).

3.2 Removal of contaminants by the newer adsorbents

3.2.1 Removal of Dyes

Fig. 5 represents the % of colour removal by two different dyes, Malachite Green and Congo Red. Almost similar removal, approximately equal to 90% can be observed by all adsorbents. However, copper-modified adsorbent demonstrated a maximum dye removal of 96% for

Malachite Green and 72% for Congo Red due to its high surface area and copper content. Moreover, absorption capacity of the WA-Cu is also quite higher 48 mg/g as compared to other adsorbents (~45 mg/g). The present study showed significantly higher adsorption capacity when compared to other reported adsorbents such as *Ricinus communis* based activated carbon, having an adsorption capacity of 27.78 mg/g[22], potato plant based activated carbon with an adsorption capacity of 27.0 mg/g[23] and *Pleurotus ostreatus* based activated carbon with 32.33 mg/g adsorption capacity[24]. The adsorption capacity for WA200, WA350, WAC200, WAC350 and WA-Cu for Congo Red removal is 29.9, 33.4, 34.7, 34.1 and 36.4 mg/g respectively. Dawood et al.[25] reported 19.18 mg/g adsorption capacity, Namasivayam et al.[26] reported an adsorption capacity of 22.44 mg/g from orange peel waste, while Nunes et al. [27] reported 14 mg/g adsorption capacity for coffee press cake based activated carbon, which is less than the adsorption capacity of developed adsorbents. Accordingly, the adsorption capacities for the newly developed materials from wood apple pulp is higher compared to many adsorbents reported earlier (Table 3). Differences in the adsorption behaviour can be attributed to nature of the dyes and varying pore size. It is clearly observed that adsorbents modified with activated charcoal showed almost similar removal capacities and adsorption rates when compared WA200. COD removal was noteworthy in both the dyes (Fig. 7). Approximately 60% COD removal was observed in the case of Malachite Green dye and around 50% COD removal was observed in the case of Congo Red for all the adsorbents, WA-Cu being an exception owing to high COD removal of 65% and 60% in both dyes respectively.

3.2.2 API pollutant (Ciprofloxacin) removal

Fig. 7 shows CIP removal using different synthesised adsorbents. WA-Cu showed 52% removal of CIP which is greater when compared to other modified adsorbents. The adsorption capacity for CIP was found to be 8.30, 7.77, 9.93, 8.36 and 10.50 mg/g for WA200, WA350, WAC200, WAC350 and WA-Cu respectively. They are significantly higher than other reported studies such as modified coal fly ash based activated carbon which showed an adsorption capacity of 1.58 mg/g[28], kaolinite with 6.3 mg/g capacity[29]and MgO nanoparticles with an adsorption capacity of 3.46 mg/g [30]. Presence of Cu nanoparticles on the surface of the adsorbent have enhanced the rate of adsorption in the case of copper modified adsorbent.

Owing to their efficiency, the exceptional functionalities of the developed adsorbents can be exploited in the polishing/tertiary treatment stage specifically suitable for low concentrations.

These biomass-derived adsorbents with their high adsorption capacity and excellent removal rates at their low costs, can be used for a limited number of cycles or even can be possibly utilised one time. Due to these reasons, regeneration which is employed in the case of expensive commercial adsorbents may not be required for these low-cost biomass derived adsorbents.

3.3 Adsorption isotherm study

To assess the adsorption performance, adsorption isotherm studies were performed, and Langmuir (Eq. 3) and Freundlich (Eq. 4) models were incorporated.

$$\frac{C_e}{q_e} = \frac{1}{q_{max}K_L} + \frac{C_e}{q_{max}} \tag{3}$$

$$ln(q_e) = lnK_F + \frac{1}{n}lnC_e \tag{4}$$

Where, C_e (mg/L) and q_e (mg/g) are equilibrium concentration and capacity respectively, q_{max} (mg/g) is maximum adsorption capacity, K_L (L/mg) is Langmuir constant, K_F (mg/g)(L/mg)$^{1/n}$ is Freundlich constant and n is heterogeneity factor.

Langmuir adsorption isotherm (Eq. 3) assumes monolayer adsorption on finite number of active sites for a homogeneous surface with q_{max} (mg/g) as the maximum monolayer adsorption capacity. Freundlich isotherm model (Eq. 4) accounts for multilayer adsorption on the surface. The data and the analysis on the fit of the models is given in Table 4 for all the different cases, on the removal of the dyes and CIP.

In the case of Malachite Green dye, all the adsorbents showed best fitting with Langmuir model with high linearization coefficient (R^2) values almost tending to unity. This indicates that homogeneous adsorption takes place on the surface of the material. The value of R_L for all the adsorbents lies in the range of 0-1 as per the calculations. This clearly indicates that adsorption is favourable[31]. The maximum theoretical adsorption capacity was 54.34 mg/g, which was comparable to that of experimental values (45 mg/g). Congo Red dye and Ciprofloxacin showed best fitting with Freundlich adsorption isotherm, which assumes multilayer adsorption on a heterogeneous surface. Freundlich adsorption constant K_F values are positive and high, which indicate a higher adsorption capacity[32]. A favourable adsorption

process requires $n > 1$ or $0 > 1/n > 1$[33]. These findings are also supported by experimental results.

3.4 Adsorption kinetics study

The rate of uptake was determined by performing pseudo first order and pseudo second order studies. Pseudo second order data show high correlation coefficient values almost close to unity (R^2=0.99) and confirm that the adsorption process follows a chemisorption process[34]. Furthermore, the maximum adsorption capacity values obtained from second order model are almost comparable to that of the experimental values (Table. 5).

3.5 Plausible mechanism of adsorption

The adsorption mechanism may be a combination of physical and chemical sorption modes. Incorporation of copper nanoparticles with biomass increased the surface area and pore size of the adsorbent leading to increase in the number of viable active sites contributing to better removal rates of the pollutant. The order of adsorption is as follows: MG > CR > CIP. The less complex structure of Malachite Green, less than the pore size in all the adsorbents owes to the higher adsorption rates when compared to other pollutant molecules like Congo Red and Ciprofloxacin which have higher degrees of complexities. FTIR analysis of the adsorbents confirmed the presence of functional groups like -OH and -COOH. Hydroxyl moieties in these groups covalently bond with the aromatic rings present in Malachite Green, which behave like H-acceptors. C=O groups present on the adsorbent surface act like e^- donors to the readily available Malachite Green molecules that act as e^- acceptors, ultimately aiding in the diffusion of the dye molecules. On the other hand, anionic dyes like Congo Red contain negatively charged ($R\text{-}SO_3^-$) groups that are electrostatically attracted to copper ions (Cu^{2+}) present on the surface of the adsorbent[35]. Hydrogen bonding between the oxygen atoms of the biomass with cationic amine groups of CIP might have led to adsorption of these molecules from the aqueous solution[36]. Altogether, the adsorption of the dye and API molecules might include various mechanisms like: (i) pore filling (ii) hydrogen bonding (iii) electrostatic interactions.

Conclusions

Newer modified biomass-derived adsorbents prepared from wood apple pulp biomass demonstrate versatility and potential in the removal of organic dyes and API pollutants. These adsorbents exhibit high efficacy even at a very low adsorbent dosage of 0.1%. All the adsorbents including modified activated carbons, copper modified adsorbents and raw biomass showed high efficiency in the removal of Malachite Green and Congo Red dyes, with impressive adsorption capacities of 48 mg/g and 36 mg/g respectively, is higher than several reported adsorbents. The equilibrium data reveals a good fit with Langmuir isotherm for Malachite Green and Freundlich isotherm in the case of Congo Red and Ciprofloxacin. Furthermore, pseudo second order kinetic model was utilised successfully to predict rates of the reaction. The results clearly highlight the potential for the use of biomass derived adsorbents in wastewater treatment, for the removal of organic pollutants from water.

Acknowledgement

VMB would like to acknowledge the funding for the research from Department of Science and technology, The Ministry of Science and Technology India, **(DST/TM/WTI/WIC/2K17/100(G))** and also Council of Scientific and Industrial Research (CSIR), Government of India (**MLP102326**).

Figures:

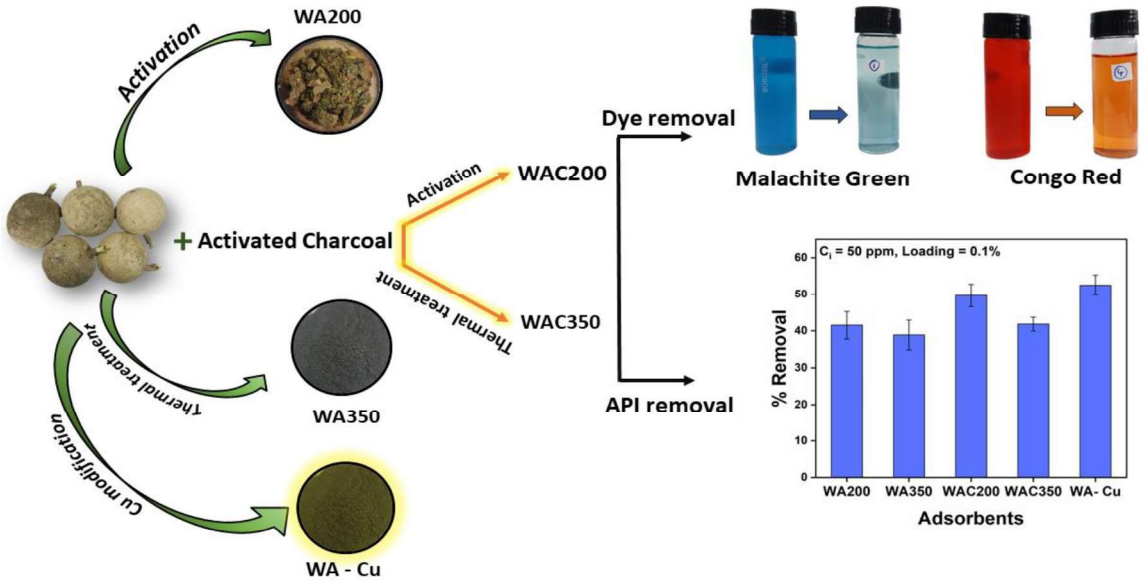

Fig. 1 Steps involved in the preparation of adsorbents

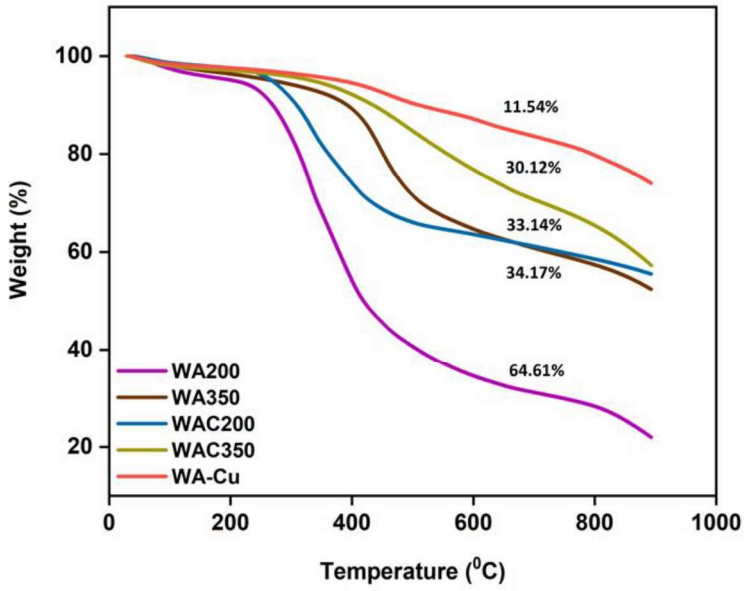

Fig. 2 TGA profiles of the adsorbents

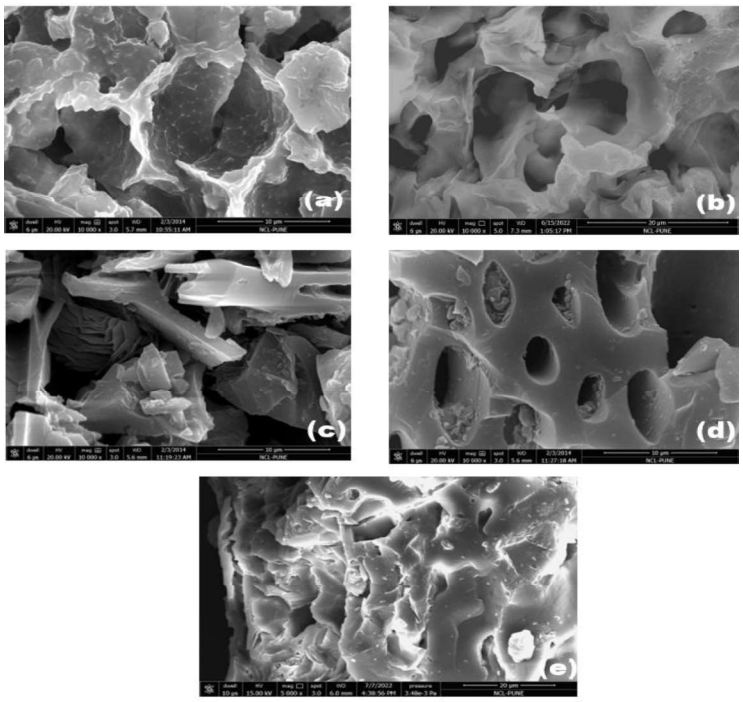

Fig. 3 FESEM images of different adsorbents, surface morphology of (a) WA200 (b) WA350 (c) WAC200 (d) WAC350 (e) WA-Cu

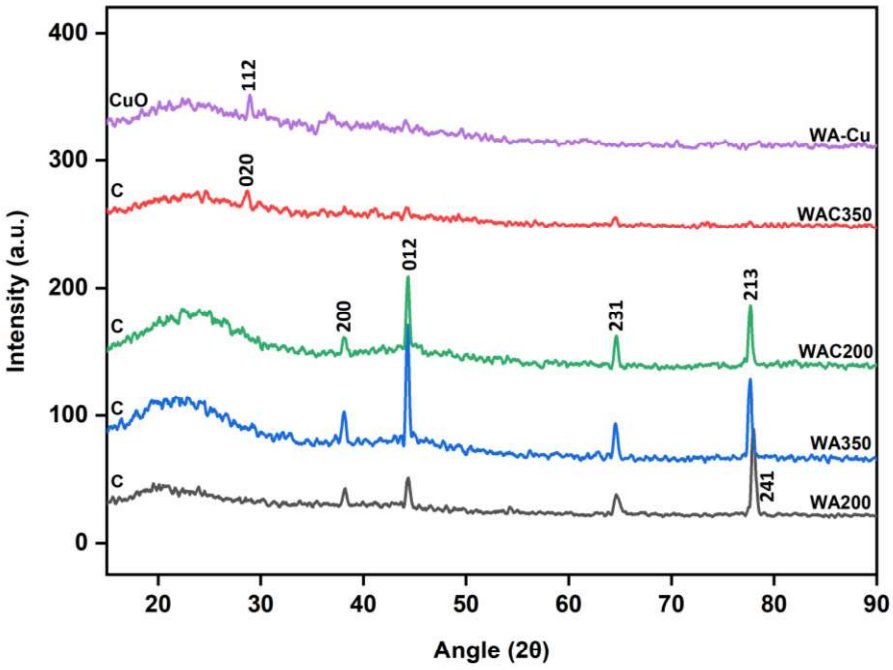

Fig. 4 XRD patterns of the adsorbents

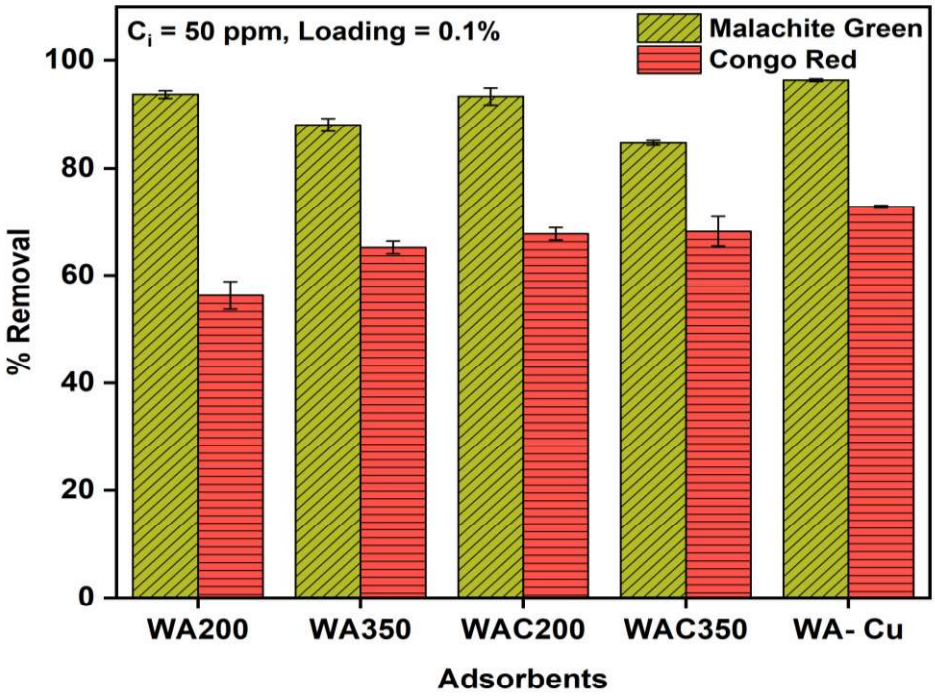

Fig. 5 Comparison of % Color removal for dyes

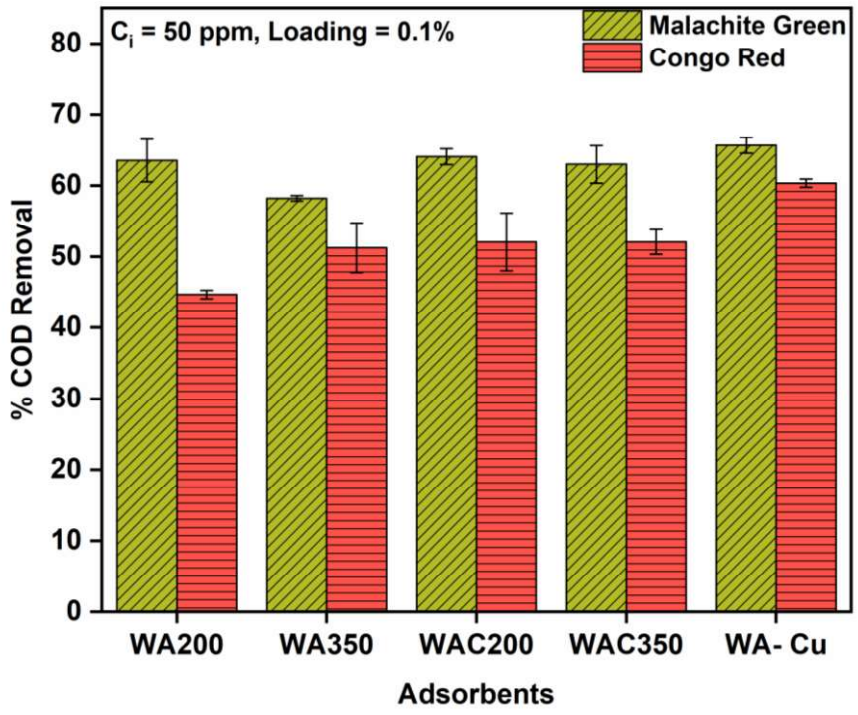

Fig. 6: Comparison of % COD removal for dyes

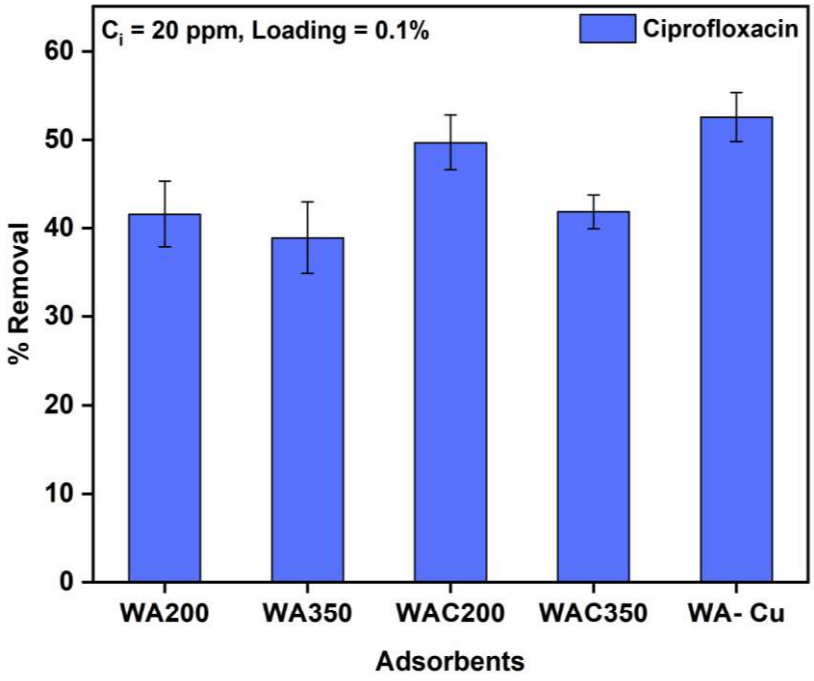

Fig. 7: % Removal of Ciprofloxacin

Tables:

Table 1: Elemental composition of the adsorbents

Element	**Composition (at%)**				
	WA200	**WA350**	**WAC200**	**WAC350**	**WA-Cu**
C	76.20	87.69	94.26	82.02	82.41
O	22.37	12.05	05.10	13.79	15.92
Ca	0.16	0.28	0.27	2.67	-
P	0.30	0.09	0.12	0.20	-
K	0.78	0.17	0.10	0.74	1.02
Cu	-	-	-	-	2.24

Table 2: Surface characteristics of adsorbents: Surface area and Pore size

Adsorbent	Surface area (m^2/g)	Pore volume (cc/g)	Pore radius (Å)
WA200	17.95	0.032	16.5
WA350	15.07	0.024	18.5
WAC200	23.30	0.055	16.6
WAC350	13.92	0.020	17.5
WA-Cu	33.31	0.022	15.6

Table 3: Comparison of adsorption capacity with different adsorbents

Material	Pollutant (Dye/CIP)	Adsorption Capacity (mg/g)	References
Ricinus communis based activated carbon	MG	27.78	[22]
Potato plant waste	MG	27.0	[23]
Pleurotus ostreatus	MG	32.33	[24]
Tamarind fruit shell	MG	1.95	[37]
Raw pine cone	CR	19.18	[25]
Waste orange peel	CR	22.44	[26]
Coffee press cake	CR	14	[27]
Aspergillus Niger	CR	14.16	[38]
Modified coal fly ash	CIP	1.58	[28]
Kaolinite	CIP	6.3	[29]
MgO nanoparticles	CIP	3.46	[30]
WA-Cu	MG	48	This work
WA-Cu	CR	36.4	This work
WA-Cu	CIP	10.5	This work

Table 4: Adsorption isotherm parameters and fit of the model

		Isotherms					
		Langmuir			Freundlich		
Adsorbent	**Dye/ API**	q_{max} *(mg/g)*	K_L *(L/mg)*	R^2	K_F *(mg/g) (L.mg)$^{1/n}$*	***n***	R^2
WA200	MG	51.54	0.89	0.97	18.51	3.04	0.95
	CR	2.30	26.48	0.98	3.15	1.45	0.99
	CIP	1.69	9.25	0.85	1.66	1.52	0.93
WA350	MG	53.19	0.86	0.97	18.45	3.01	0.96
	CR	2.56	16.37	0.85	2.56	1.37	0.94
	CIP	1.95	6.94	0.77	1.77	1.61	0.90
WAC200	MG	40.81	1.18	0.96	17.90	2.98	0.93
	CR	3.58	10.68	0.93	4.13	1.72	0.98
	CIP	1.57	9.88	0.83	1.56	1.49	0.90
WAC350	MG	54.34	0.88	0.97	19.36	3.15	0.94
	CR	3.54	11.20	0.91	3.88	1.63	0.97
	CIP	1.96	6.82	0.77	1.76	1.61	0.90
WA-Cu	MG	33.33	2.27	0.92	21.85	2.54	0.73
	CR	2.92	14.40	0.90	3.19	1.49	0.96
	CIP	1.74	8.55	0.82	1.69	1.55	0.92

Table 5: Kinetic model parameters and fit of the model

			pseudo first order			pseudo second order		
Adsorbent	**Dye/CIP**	q_{exp} *(mg/ g)*	q_{thr} *(mg/g)*	k_1 *(min^{-1})*	R^2	q_{thr} *(mg/g)*	k_2 *(g/mg/min)*	R^2
WA200	MG	46.8	25.73	0.001	0.89	48.30	0.005	0.99
	CR	29.9	1.88	0.001	0.36	42.73	0.003	0.99
	CIP	8.30	0.92	-1.72E-05	0.58	13.17	0.008	0.99
WA350	MG	44.0	15.42	0.0006	0.39	47.16	0.003	0.99

	CR	33.4	12.05	0.0005	0.70	38.46	0.002	0.99
	CIP	7.77	1.47	8.82E-05	0.28	13.44	0.074	0.98
WAC200	MG	46.6	9.09	0.0009	0.79	50.00	0.004	0.99
	CR	34.7	13.00	0.0005	0.85	39.52	0.002	0.98
	CIP	9.93	0.93	0.0013	0.82	13.17	0.008	0.99
WAC350	MG	42.3	12.84	0.0006	0.42	48.54	0.005	0.99
	CR	34.1	242.08	0.0012	0.81	38.02	0.008	0.99
	CIP	8.36	2.17	0.0004	0.62	14.74	0.004	0.97
WA-Cu	MG	48.1	20.28	0.0058	0.95	49.01	0.004	0.99
	CR	36.4	4.70	0.0004	0.78	37.45	0.011	0.99
	CIP	10.5	5.38	0.0003	0.92	10.26	0.009	0.98

References

1. K. Balapure, V.M. Bhandari, J. of ISAS 2,3, 2023.
2. R. Gothwal, T. Shashidhar, Clean Soil Air Water 43, 479, 2015.
3. V. V. Ranade V.M. Bhandari, Industrial Wastewater Treatment, Recycling and Reuse. Elsevier, 06975, 2014.
4. O.A.A, Eletta, S.I. Mustapha, O.A. Ajayi, A.T. Ahmed, Niger. J. Technol. Dev. 15, 26, 2018.
5. K. Sharma, M. Chethana, V.M. Bhandari, Sorokhaibam, Laxmi Gayatri, V.V. Ranade, D.J. Killedar, J. ISAS 1, 3, 2023.
6. O.S. Bello, M.A. Ahmad, Sep Sci Technol 47, 903, 2012.
7. A. Sharma, Z.M. Siddiqui, S. Dhar, P. Mehta, D. Pathania, . Sep. Sci. Technol. 54, 916, 2019.
8. T.A. Gad-Allah, M.E.M, Ali, M.I. Badawy, J. Hazard. Mater. 186, 751, 2011.
9. S. Shi, Y. Fan, Y. Huang, Ind. Eng. Chem. Res. 52, 2604, 2013.
10. L.G. Sorokhaibam, V. M. Bhandari, M.S. Salvi, J. S. jain, S.D. Hadawale, V.V. Ranade Ind. Eng. Chem. Res. 54, 11844, 2015.
11. A.A. Ahmad, A.T.M, N.K.E. Din Yahaya, M.A., A. Khasri, M.A. Ahmad, Arab. J. Chem.13, 6887, 2020.
12. N.K. Mondal, S. Kar, Appl.Water Sci. 8, 157, 2018.
13. S. Lahreche, I. Moulefera, A. El Kebir, L. Sabantina, M. Kaid, Benyoucef, A. Fibers,

10, 7, 2022.

14. P.E. Jagadeesh Babu, V. Kumar, R. Visvanathan, J. Chem. Eng. 5, 465, 2009.
15. T.T. Dao, T. Hong-tham T. Nguyen, C.N. Duyen Thi, T.N. Hanh , H. T.T. Nguyen, S.Y. Trung Do, L.O.C, Huu, T.T. Nguyen, T.D. Nguyen, L.G.bach, Cellul. Chem. Technol. 54, 811, 2020.
16. R.A. Teixeira, E.C. Lima, A.D. Benetti,P. Thue, R. N, Mohamed, A. aved. Environ. Sci. Pollut. Res.2022.
17. N.S. Kumar, H. M. Shaikh, M. Asif, E.H. Al-Ghurabi, Sci. Rep. 11, 2586, 2021.
18. S. Prashanth, C. Subramaniam, Bharatwaj, N. R. Akshykumar, K. Nithya, Int. J. Environ. Sci. Technol. 19,1247, 2022.
19. M.F. Mohamad Yusop, M.A. Ahmad, N.A. Rosli, N. Gonawan, Abdullah, S.J. Malaysian J. Fundam. Appl. Sci. 17, 95, 2021.
20. A.H. Wazir, I.U. Wazir, A.M. Wazir, Energy Sources, Part A: Recovery Utility Environ. Effects, 1, 2020.
21. M. Shahrashoub, S. Bakhtiari, Microporous Mesoporous Mater. 311, 110692, 2021.
22. T. Santhi, S. Manonmani, T. Smitha, J. Hazard. Mater. 179, 178, 2010.
23. N. Gupta, A. K. Kushwaha, M.C. Chattopadhyaya, Arab. J. Chem. 9, 707, 2016.
24. Z. Chen, H. Deng, C, Chen, Y. Yang, Xu, H.J. Environ. Heal. Sci. Eng. 12, 1, 2014.
25. S. Dawood, T.K. Sen, Water Res. 46, 1933, 2012.
26. C. Namasivayam, N. Muniasamy, K. Gayatri, M. Rani, K. Rangnathan Bioresour. Technol. 57, 37, 1996.
27. A.A. Nunes, A.S. Franca, L.S. Oliveira, Bioresour. Technol. 100, 1786, 2009.
28. C.L. Zhang, G.L. Qiao, F. Zhao, Y. Wang, J. Mol. Liq. 163, 53, 2011.
29. Z. Li, H. Hong, L. Liao, Ackley, C.J., Schulz, C.J, schulz, L.A, MacDonald, R. Mihelich, A.L, Emard, S. M. Colloids Surfaces B Biointerfaces 88, 339, 2011.
30. N. Khoshnamvand, S. Ahmadi, F.K. Mostafapour, J. Appl. Pharm. Sci. 7,79, 2017.
31. G.M. Yalvaç, B. Bayrak, Desalin Water Treat 177, 176, 2020.
32. O. Tunç, H. Tanac, Z. Aksu, J. Hazard. Mater. 163, 187, 2009.
33. W. Konicki, M. Aleksandrzak, D. Moszyński, E. Mijowska, J. Colloid Interface Sci. 496,188, 2017.
34. S.A. Patil, U.P. Suryawanshi, N.S. Harale, S.K. Patil, Vadiyar, S.K, Luwang, M.N, Anuse, Kim, J.H., S.S. Kolekar, . Int. J. Environ. Anal. Chem. 1, 2020.
35. E. Sharifpour, E. Alipanahpour, A. Asfaram, Ghaedi, M, Goudarzi, A. Appl. Organomet. Chem. 33, 4768, 2019.

36. A. Maged, S. Kharbish, I.S. Ismael, A. Bhatnagar, Environ. Sci. Pollut. Res. 27, 32980, 2020.
37. P. Saha, S. Chowdhury, S. Gupta, Indresh, K. Clean Soil Air Water 38, 437, 2010.
Y. Fu, T. Viraraghavan, Adv. Environ. Res. 7, 239, 2002.